PROCEEDINGS A

royalsocietypublishing.org/journal/rspa

Research

Cite this article: Mucalica A, Pelinovsky DE. 2022 Solitons on the rarefaction wave background via the Darboux transformation. *Proc. R. Soc. A* **478**: 20220474. https://doi.org/10.1098/rspa.2022.0474

Received: 7 July 2022
Accepted: 2 November 2022

Subject Areas:
applied mathematics, mathematical modelling, fluid mechanics

Keywords:
Korteweg-de Vries equation, rarefaction wave, Darboux transformation, transmitted solitons, trapped solitons, eigenvalues, resonant poles

Author for correspondence:
Dmitry E. Pelinovsky
e-mail: dmpeli@math.mcmaster.ca

Solitons on the rarefaction wave background via the Darboux transformation

Ana Mucalica[1] and Dmitry E. Pelinovsky[1,2]

[1]Department of Mathematics and Statistics, McMaster University, Hamilton, L8S 4K1 Ontario, Canada
[2]Institute of Applied Physics RAS, Nizhny Novgorod 603950, Russia

DEP, 0000-0001-5812-440X

Rarefaction waves and dispersive shock waves are generated from the step-like initial data in many nonlinear evolution equations including the classical example of the Korteweg–de Vries (KdV) equation. When a solitary wave is injected on the step-like initial data, it is either transmitted over or trapped inside the rarefaction wave background. We show that the transmitted soliton can be obtained by using the Darboux transformation for the KdV equation. On the other hand, we show with the help of numerical simulations that the trapped soliton disappears in the long-time dynamics of the rarefaction wave.

1. Introduction

The Korteweg–de Vries (KdV) equation is a classical model for long surface gravity waves of small amplitude propagating unidirectionally over shallow water of uniform depth [1]. The normalized version of the KdV equation takes the form

$$u_t + 6uu_x + u_{xxx} = 0, \tag{1.1}$$

where t is the evolution time, x is the spatial coordinate for the wave propagation and u is the fluid velocity. The KdV equation has predominantly been studied on spatial domains with either decaying or periodic boundary conditions. However, due to many applications, e.g. the tidal bores or the earthquake-generated waves [2], it is also relevant to consider the initial value problem with the step-like boundary conditions:

$$\lim_{x\to-\infty} u(t,x) = 0 \quad \text{and} \quad \lim_{x\to+\infty} u(t,x) = c^2, \tag{1.2}$$

where $c^2 > 0$ is a constant.

THE ROYAL SOCIETY PUBLISHING

Evolution of the step-like data results in the appearance of a rarefaction wave (RW) if t advances to positive times or a dispersive shock wave (DSW) if t advances to negative times [3]. In what follows, we will consider the initial value problem (1.2) for the RW in positive time $t > 0$ since the analysis for negative time $t < 0$ is similar [4].

The interaction of waves with a mean flow is an important and well-established problem of fluid mechanics, and it has been an active area of research. An excellent account on the hydrodynamics of optical soliton tunnelling is given in ref. [5], where a localized, depression wave (known as the dark soliton) of the one-dimensional defocusing nonlinear Schrödinger (NLS) equation interacted with either RW or DSW. Other examples of the interaction between localized solitary waves with large-scale, time-varying dispersive mean flows were studied in ref. [6] for the modified KdV equation and in ref. [7] for the Benjamin–Bona–Mahony equation. A dual problem was the interaction of a linear wavepacket (modulated waves) with the step-like initial data [8]. Both transmission and trapping conditions of a small amplitude, linear, dispersive wave propagating through an expansion (RW) or a undular bore (DSW) were explained by using the Whitham modulation theory [9–11].

Focusing versions of the same problem were also considered in the cubic NLS equation [12,13] and in the modified KdV equation [14]. Due to modulational instability, solitary waves, breathers, and rogue waves were generated from the step-like initial data.

The initial value problem for the KdV equation can be analyzed by means of the inverse scattering transform (IST) method [15], pioneered in refs. [16,17], which relates a solution of the KdV equation (1.1) to the spectrum of the stationary Schrödinger equation:

$$\mathcal{L}v = \lambda v \quad \text{and} \quad \mathcal{L} := -\frac{\partial^2}{\partial x^2} - u, \tag{1.3}$$

and the time evolution equation:

$$\frac{\partial v}{\partial t} = \mathcal{M}v \quad \text{and} \quad \mathcal{M} := -3u_x - 6u\frac{\partial}{\partial x} - 4\frac{\partial^3}{\partial x^3}. \tag{1.4}$$

The compatibility condition for the time-independent spectral parameter λ yields the KdV equation (1.1) for $u = u(t, x)$.

The IST method is usually applied on the infinite line for the initial data that decay to zero sufficiently fast at infinity. In this case, the time evolution of the KdV equation (1.1) from arbitrary initial data leads to a generation of finitely many interacting solitons and the dispersive waves [18]. Solitons correspond to isolated eigenvalues of the discrete spectrum of the stationary Schrödinger equation (1.3) and the dispersive waves correspond to the continuous spectrum.

For the step boundary conditions (1.2), the dynamics of the KdV equation (1.1) are more interesting. In addition to the RW generated by the step boundary conditions for $t > 0$, a finite number of solitary waves can appear from bumps in the initial data. Depending on the amplitude of these bumps, they either evolve into large amplitude solitary waves propagating over the RW background or into small amplitude solitary waves trapped by the RW [4].

The spectrum of the stationary Schrödinger equation (1.3) for the step-like boundary conditions (1.2) was analyzed in ref. [19], where it was shown that the transmitted soliton corresponds to an isolated real eigenvalue. Regarding the trapped soliton, it was related to the so-called pseuso-embedded eigenvalue located near a specific point inside the continuous spectrum. It was understood that this 'pseuso-embedded eigenvalue' did not correspond to a true embedded eigenvalue with exponentially decaying eigenfunctions; however, details of where such 'eigenvalues' were located were not given.

The rigorous IST method was applied to the KdV equation with the step-like boundary conditions in [20,21]. Compared to (1.2) for the RW, the case of DSW was considered with zero boundary conditions as $x \to +\infty$. N solitons scatter towards $+\infty$ as $t \to +\infty$ as regular KdV solitons with appropriately chosen phase shifts. The case of trapped solitons did not appear in the IST formalism.

Here, we will analyze the two scenarios of transmitted or trapped solitary waves similar to ref. [19] but in more detail. Our principal results can be summarized as follows:

(1) The transmitted solitary wave can be generated by using the Darboux transformation of the KdV equation. The Darboux transformation determines the different spatial decay rates of the solitary wave for both $x \to -\infty$ and $x \to +\infty$ by the location of an isolated real eigenvalue of the stationary Schrödinger equation (1.3).
(2) The trapped solitary wave does not actually exist as a proper soliton of the KdV equation. The initial condition with a 'pseudo-embedded eigenvalue' is associated with resonant poles of the stationary Schrödinger equation, which are located off the real axis and correspond to spatially decaying eigenfunctions at one infinity and growing at the other infinity.
(3) By using numerical experiments, we show that the asymptotic amplitude of the transmitted solitary wave is determined by the initial amplitude, whereas the amplitude of the trapped solitary wave decays to the amplitude of the RW background so that the trapped solitary wave becomes invisible from the RW background for longer times.

(a) Organization of the paper

Section 2 reviews the scattering data and their time evolution for the class of solutions satisfying the boundary conditions (1.2). Section 3 presents details of the direct scattering for two examples of the initial data: the step function and a solitary wave on the step function. Section 4 presents a construction of a transmitted solitary wave on the RW background via Darboux transformation. Section 5 describes numerical simulations which illustrate that a trapped solitary wave disappears inside the RW background as time evolves. Section 6 gives a summary of our findings and lists open questions.

(b) Notations

We denote the Heaviside step function by H. The square root function $\sqrt{z}$ for $z \in \mathbb{C}$ is defined according to the principal branch such that $\mathrm{Arg}(\sqrt{z}) \in [0, \pi)$ for every $z \in \mathbb{C}$ with $\mathrm{Arg}(z) \in [0, 2\pi)$.

2. Direct scattering transform and the time evolution

Here, we review the spectral data and their time evolution in the solutions of the linear equations (1.3) and (1.4) for the potential $u = u(t, x)$ satisfying the boundary conditions (1.2). We assume that $u(t, x) \to c^2 H(x)$ as $|x| \to \infty$ sufficiently fast so that all formal expressions can be rigorously justified with Levinson's theorem for differential equations whose variable coefficients are integrable perturbations of the constant coefficients.

The linear equation (1.4) can be rewritten in the following form:

$$\frac{\partial v}{\partial t} = (4\lambda - 2u)\frac{\partial v}{\partial x} + (u_x + \gamma)v, \tag{2.1}$$

where we have used $v_{xxx} = -(u + \lambda)v_x - u_x v$ from the Schrödinger equation (1.3) and have added the parameter γ by the transformation $v \mapsto v\, \mathrm{e}^{-\gamma t}$.

We are looking for the spatially bounded non-zero solutions $v = v(t, x)$. Existence of such solutions depend on the values of the spectral parameter λ and should be performed separately in three regions:

$$(0, \infty), \quad (-c^2, 0), \quad \text{and} \quad \lambda \in (-\infty, -c^2).$$

The border cases $\lambda = 0$ and $\lambda = -c^2$ can also be included in the consideration but will be omitted to keep the presentation concise.

royalsocietypublishing.org/journal/rspa Proc. R. Soc. A 478: 20220474

(a) Case $\lambda \in (0, \infty)$

We parameterize positive λ as $\lambda = k^2$ with $k > 0$ and introduce

$$\varkappa := \sqrt{c^2 + k^2}.$$

such that $\varkappa > 0$. One solution of the stationary Schrödinger equation (1.3) with $u(t,x) \to c^2 H(x)$ as $|x| \to \infty$ is given by $\phi(t,x;k)$ satisfying

$$\phi(t,x;k) \to \begin{cases} \mathrm{e}^{-ikx}, & x \to -\infty, \\ a(t;k)\,\mathrm{e}^{-i\varkappa x} + b(t;k)\,\mathrm{e}^{i\varkappa x}, & x \to +\infty, \end{cases} \tag{2.2}$$

where the coefficients $a(t;k)$ and $b(t;k)$ are referred to as the scattering data. The second linearly independent eigenfunction is given by $\phi(t,x;-k)$. Both solutions are oscillatory on $\mathbb{R}$ and do not decay to zero at infinity.

Substituting the asymptotics $\phi(t,x;k) \to \mathrm{e}^{-ikx}$ and $u(t,x) \to 0$ as $x \to -\infty$ into (2.1), we obtain the definition of γ:

$$0 = \gamma\,\mathrm{e}^{-ikx} - 4ik^3\,\mathrm{e}^{-ikx} \Rightarrow \gamma = 4ik^3. \tag{2.3}$$

Substituting the asymptotics $\phi(t,x;k) \to a(t;k)\,\mathrm{e}^{-i\varkappa x} + b(t;k)\,\mathrm{e}^{i\varkappa x}$ and $u(t,x) \to c^2$ as $x \to +\infty$ into (2.1) and using the same value of γ from (2.3), we obtain

$$\frac{\mathrm{d}a}{\mathrm{d}t} = i(4k^3 - 4k^2\varkappa + 2c^2\varkappa)a$$

and

$$\frac{\mathrm{d}b}{\mathrm{d}t} = i(4k^3 + 4k^2\varkappa - 2c^2\varkappa)b$$

from which the exact solution is given by

$$a(t;k) = a(0;k)\,\mathrm{e}^{i(4k^2(k-\varkappa)+2c^2\varkappa)t} \quad \text{and} \quad b(t;k) = b(0;k)\,\mathrm{e}^{i(4k^2(k+\varkappa)-2c^2\varkappa)t}. \tag{2.4}$$

Compared to the case of $c = 0$, it is no longer true that $a(t;k)$ is constant in t.

(b) Case $\lambda \in (-c^2, 0)$

We parameterize negative λ by $\lambda = -\mu^2$ with $\mu \in (0, c)$ and introduce

$$\varkappa := \sqrt{c^2 - \mu^2},$$

such that $\varkappa > 0$. For the sake of notations, we redefine $\phi(t,x;k)$, $a(t;k)$ and $b(t;k)$ for $k = i\mu$ with $\mu > 0$ as $\phi(t,x;\mu)$, $a(t;\mu)$ and $b(t;\mu)$. We do not assume here any analyticity of the eigenfunctions and scattering data in k. The only bounded solution as $x \to -\infty$ is obtained from (2.2) with $k = i\mu$ as $\phi(t,x;\mu)$ satisfying

$$\phi(t,x;\mu) \to \begin{cases} \mathrm{e}^{\mu x}, & x \to -\infty, \\ a(t;\mu)\,\mathrm{e}^{-i\varkappa x} + b(t;\mu)\,\mathrm{e}^{i\varkappa x}, & x \to +\infty. \end{cases} \tag{2.5}$$

Time evolution of the scattering data is obtained from (2.4) with the same change $k = i\mu$:

$$a(t;\mu) = a(0;\mu)\,\mathrm{e}^{(4\mu^2(\mu+i\varkappa)+2ic^2\varkappa)t} \quad \text{and} \quad b(t;\mu) = b(0;\mu)\,\mathrm{e}^{(4\mu^2(\mu-i\varkappa)-2ic^2\varkappa)t}. \tag{2.6}$$

The second linearly independent solution $\phi(t,x;-\mu)$ is unbounded as $x \to -\infty$. Note that $\phi(t,x;\mu)$ decays to zero as $x \to -\infty$ but is oscillatory as $x \to +\infty$.

(c) Case $\lambda \in (-\infty, -c^2)$

We use the same parameterization $\lambda = -\mu^2$ with $\mu > c$ and introduce

$$\nu := \sqrt{\mu^2 - c^2},$$

such that $\nu > 0$. The only bounded solution as $x \to -\infty$ is obtained from (2.5) with $\varkappa = i\nu$, so that $\phi(t, x; \mu)$ satisfies

$$\phi(t, x; \mu) \to \begin{cases} e^{\mu x} & x \to -\infty, \\ a(t; \mu)\, e^{\nu x} + b(t; \mu)\, e^{-\nu x} & x \to +\infty. \end{cases} \tag{2.7}$$

The second linearly independent solution $\phi(t, x; -\mu)$ is unbounded as $x \to -\infty$. If $a(t; \mu) \neq 0$, then $\phi(t, x; \mu)$ is unbounded as $x \to +\infty$. However, if $a(t; \mu_0) = 0$ for some $\mu_0 \in (c, \infty)$, then the eigenfunction $\phi(t, x; \mu_0)$ is bounded and exponentially decaying as $|x| \to \infty$. The corresponding eigenfunction satisfies

$$\phi(t, x; \mu_0) \to \begin{cases} e^{\mu_0 x}, & x \to -\infty, \\ b_0(t)\, e^{-\nu_0 x}, & x \to +\infty, \end{cases}$$

where $\nu_0 := \sqrt{\mu_0^2 - c^2}$ and $b_0(t)$ satisfies the time evolution that follows from (2.6):

$$b_0(t) = b_0(0)\, e^{(4\mu_0^2(\mu_0 + \nu_0) + 2c^2\nu_0)t}.$$

Note that $\phi(t, x; \mu_0)$ is exponentially decaying as $x \to \pm\infty$ with two different decay rates: μ_0 at $-\infty$ and ν_0 at $+\infty$.

Remark 2.1. We say that $\lambda_0 = -\mu_0^2$ is *an isolated eigenvalue* of the stationary Schrödinger equation (1.3) if $a(t; \mu_0) = 0$ for $\mu_0 \in (c, \infty)$ and we say that $[-c^2, \infty)$ is *the continuous spectrum* of the stationary Schrödinger equation (1.3).

3. Examples of the step-like initial conditions

Here, we solve the scattering problem for two simplest initial conditions satisfying the boundary conditions (1.2). Since the time evolution of the scattering data is not considered, we drop t from the list of arguments.

(a) Case of the step function $u_0(x) = c^2 H(x)$

For $\lambda \in (0, \infty)$, the eigenfunction is given by (2.2), where the superposition of exponential functions hold for every $x < 0$ and $x > 0$, not just in the limits $x \to -\infty$ and $x \to +\infty$. Since $\phi(x)$ and $\phi'(x)$ must be continuous at $x = 0$, we derive the system of linear equations for $a(k)$ and $b(k)$:

$$1 = a(k) + b(k) \quad \text{and} \quad -ik = i\varkappa b(k) - i\varkappa a(k), \tag{3.1}$$

where $\varkappa = \sqrt{c^2 + k^2}$. The linear system (3.1) admits a unique solution given by

$$a(k) = \frac{\varkappa + k}{2\varkappa} \quad \text{and} \quad b(k) = \frac{\varkappa - k}{2\varkappa}. \tag{3.2}$$

Similarly, for $\lambda \in (-c^2, 0)$, the scattering data $a(\mu)$ and $b(\mu)$ are obtained from (3.2) by substituting $k = i\mu$ with $\mu > 0$:

$$a(\mu) = \frac{\varkappa + i\mu}{2\varkappa} \quad \text{and} \quad b(\mu) = \frac{\varkappa - i\mu}{2\varkappa}, \tag{3.3}$$

where $\varkappa = \sqrt{c^2 - \mu^2}$. No zeros of $a(\mu)$ exists for $\lambda \in (-\infty, -c^2)$ since $a(\mu)$ is given by the same expression (3.3) but with $\varkappa = i\sqrt{\mu^2 - c^2}$ and $\sqrt{\mu^2 - c^2} + \mu > 0$. The spectrum of the stationary Schrödinger equation (1.3) is purely continuous.

Remark 3.1. The step function can be replaced by the smooth function

$$u_0(x) = \frac{1}{2}c^2\,[1 + \tanh(\varepsilon x)], \quad \varepsilon > 0. \tag{3.4}$$

Exact solutions for the scattering data $a(k)$ and $b(k)$ associated with u_0 in (3.4) are available in the literature [22]. The spectrum of the stationary Schrödinger equation (1.3) is also purely continuous. We use (3.4) instead of $c^2H(x)$ in numerical computations to reduce the numerical noise generated by the step function.

(b) Case of a soliton on the step function

We consider a linear superposition of a soliton and the step function:

$$u_0(x) = 2\mu_0^2\,\mathrm{sech}^2(\mu_0(x - x_0)) + c^2H(x), \tag{3.5}$$

where $\mu_0 > 0$ is the soliton parameter and $x_0 < 0$ is chosen to ensure that the soliton is located to the left of the step function. The direct scattering problem for the initial condition (3.5) was solved in ref. [19], and here, we extend the solution with more details.

The spectral problem (1.3) with $u = u_0$ can be solved exactly [22]. For $x < 0$, the exact solution for $\phi(x;k)$ satisfying $\phi(x;k) \to \mathrm{e}^{-\mathrm{i}kx}$ as $x \to -\infty$ is given by

$$\phi(x;k) = \mathrm{e}^{-\mathrm{i}kx}\left[1 - \frac{i\mu_0}{k + i\mu_0}\,\mathrm{e}^{\mu_0(x-x_0)}\,\mathrm{sech}(\mu_0(x - x_0))\right], \quad x < 0.$$

Similarly for $x > 0$, the exact solution for $\psi(x;k)$ satisfying $\psi(x;k) \to \mathrm{e}^{\mathrm{i}\varkappa x}$ as $x \to +\infty$ is given by

$$\psi(x;k) = \mathrm{e}^{\mathrm{i}\varkappa x}\left[1 - \frac{i\mu_0}{\varkappa + i\mu_0}\,\mathrm{e}^{-\mu_0(x-x_0)}\,\mathrm{sech}(\mu_0(x - x_0))\right], \quad x > 0.$$

The scattering data $a(k)$ and $b(k)$ in the representation (2.2) can be found from the scattering relation:

$$\phi(x;k) = a(k)\overline{\psi}(x;k) + b(k)\psi(x;k), \quad x \in \mathbb{R},$$

where $\overline{\psi}(x;k)$ is obtained from $\psi(x;k)$ by reflection $\varkappa \mapsto -\varkappa$. Since the Wronskian $W(\psi_1, \psi_2)$ of any two solutions ψ_1 and ψ_2 of the stationary Schrödinger equation (1.3) is independent of x, the scattering coefficient $a(k)$ can be obtained from the formula:

$$a(k) = \frac{W(\phi(x;k), \psi(x;k))}{W(\bar{\psi}(x;k), \psi(x;k))}, \quad x \in \mathbb{R}, \tag{3.6}$$

where we are free to choose $x = 0$ in (3.6). Hence, we compute

$$\begin{aligned} W(\bar{\psi}, \psi)|_{x=0} &= 2i\varkappa\left(1 + \frac{i\mu_0\,\mathrm{e}^{\mu_0 x_0}\,\mathrm{sech}(\mu_0 x_0)}{\varkappa - i\mu_0}\right)\left(1 - \frac{i\mu_0\,\mathrm{e}^{\mu_0 x_0}\,\mathrm{sech}(\mu_0 x_0)}{\varkappa + i\mu_0}\right) \\ &\quad + \frac{i\mu_0^2\,\mathrm{sech}^2(\mu_0 x_0)}{\varkappa - i\mu_0}\left(1 - \frac{i\mu_0\,\mathrm{e}^{\mu_0 x_0}\,\mathrm{sech}(\mu_0 x_0)}{\varkappa + i\mu_0}\right) \\ &\quad + \frac{i\mu_0^2\,\mathrm{sech}^2(\mu_0 x_0)}{\varkappa + i\mu_0}\left(1 + \frac{i\mu_0\,\mathrm{e}^{\mu_0 x_0}\,\mathrm{sech}(\mu_0 x_0)}{\varkappa - i\mu_0}\right) \\ &= 2i\varkappa \end{aligned}$$

and

$$W(\phi,\psi)|_{x=0} = i(\varkappa+k)\left(1-\frac{i\mu_0\,\mathrm{e}^{\mu_0 x_0}\,\mathrm{sech}(\mu_0 x_0)}{\varkappa+i\mu_0}\right)\left(1-\frac{i\mu_0\,\mathrm{e}^{\mu_0 x_0}\,\mathrm{sech}(\mu_0 x_0)}{\varkappa+i\mu_0}\right)$$
$$+\frac{i\mu_0^2\,\mathrm{sech}^2(\mu_0 x_0)}{\varkappa+i\mu_0}\left(1-\frac{i\mu_0\,\mathrm{e}^{-\mu_0 x_0}\,\mathrm{sech}(\mu_0 x_0)}{k+i\mu_o}\right)$$
$$+\frac{i\mu_0^2\,\mathrm{sech}^2(\mu_0 x_0)}{k+i\mu_0}\left(1-\frac{i\mu_0\,\mathrm{e}^{\mu_0 x_0}\,\mathrm{sech}(\mu_0 x_0)}{\varkappa+i\mu_0}\right)$$
$$=\frac{i(\varkappa+k)(\varkappa k+\mu_0^2+i\mu_0(\varkappa-k)\tanh(\mu_0 x_0))}{(\varkappa+i\mu_0)(k+i\mu_0)},$$

which yields

$$a(k)=\frac{(\varkappa+k)(\varkappa k+\mu_0^2+i\mu_0(\varkappa-k)\tanh(\mu_0 x_0))}{2\varkappa(\varkappa+i\mu_0)(k+i\mu_0)}. \tag{3.7}$$

This expression coincides with (A6) in [19] up to notations.

Although the previous expressions were obtained for $\lambda=k^2>0$ with $k\in\mathbb{R}$, the scattering coefficient $a(k)$ can be continued analytically for $k\in\mathbb{C}$ with $\mathrm{Im}(k)\geq 0$. However, $k=ic$ is a branch point for the square root function for $\varkappa:=\sqrt{c^2+k^2}$. The branch cuts can be defined at our disposal on the imaginary axis, $\mathrm{Re}(k)=0$, for which $\mathrm{Im}(k)$ takes values on

$$\text{either } [-c,c] \quad \text{or } (-\infty,-c]\cup[c,\infty).$$

We are looking for zeros of $a(k)$ for $\mathrm{Im}(k)>0$ for which $\phi(x;k)\to 0$ as $x\to-\infty$.

— If $a(k_0)=0$ with $\mathrm{Im}(k_0)\in(c,\infty)$ corresponds to $\varkappa_0:=\sqrt{c^2+k_0^2}$ satisfying $\mathrm{Im}(\varkappa_0)>0$, then $\phi(x;k_0)=b_0\psi(x;k_0)\to 0$ as $x\to+\infty$. This yields *the eigenvalue* $\lambda_0:=k_0^2$ of the spectral problem (1.3), for which the branch cut can be chosen for $\mathrm{Re}(k)=0$ and $\mathrm{Im}(k)\in[-c,c]$. In this case, the spectral theory of the Schrödinger equation (1.3) implies that $\mathrm{Re}(k_0)=0$ and $\mathrm{Re}(\varkappa_0)=0$.

— If $a(k_0)=0$ with $\mathrm{Im}(k_0)\in(0,c)$ corresponds to $\varkappa_0:=\sqrt{c^2+k_0^2}$ satisfying $\mathrm{Re}(\varkappa_0)>0$ and $\mathrm{Im}(\varkappa_0)<0$, then $\phi(x;k_0)=b_0\psi(x;k_0)\to\infty$ as $x\to+\infty$. In this case, we say that $\lambda_0:=k_0^2$ is *the resonant pole* of the spectral problem (1.3). The branch cut can be chosen for $\mathrm{Re}(k)=0$ and $\mathrm{Im}(k)\in(-\infty,-c]\cup[c,\infty)$, and $\mathrm{Re}(k_0)$ is not generally zero.

Remark 3.2. The coefficient b_0 in $\phi(x;k_0)=b_0\psi(x;k_0)$ for which $a(k_0)=0$ cannot be associated with $b(k_0)$ because the scattering coefficient $b(k)$ is not analytically continued off the real axis unlike the scattering coefficient $a(k)$.

We are now in position to analyze zeros of $a(k)$ given by (3.7). The following proposition presents the main outcome of this analysis.

Proposition 3.3. *For sufficiently large negative x_0, an isolated eigenvalue $\lambda_0\in(-\infty,-c^2)$ persists near $-\mu_0^2$ if $\mu_0\in(c,\infty)$, whereas the embedded eigenvalue $\lambda_0\in(-c^2,0)$ moves to a resonant pole with $\mathrm{Re}(k_0)<0$ and $\mathrm{Im}(\varkappa_0)<0$ if $\mu_0\in(0,c)$.*

Proof. Since $\varkappa+k\neq 0$, it follows from (3.7) that $a(k)=0$ if and only if k is the root of the following transcendental equation:

$$\varkappa k+\mu_0^2+i\mu_0(\varkappa-k)\tanh(\mu_0 x_0)=0. \tag{3.8}$$

The algebraic equation (3.8) is factorized in the limit $x_0\to-\infty$ as $(\varkappa+i\mu_0)(k-i\mu_0)=0$. Hence, there exists a simple root $k=i\mu_0$ in the limit $x_0\to-\infty$. If $\mu_0\in(c,\infty)$, this root corresponds to an isolated eigenvalue $\lambda=-\mu_0^2\in(-\infty,-c^2)$; however, if $\mu_0\in(0,c)$, the root corresponds to an embedded eigenvalue $\lambda=-\mu_0^2\in(-c^2,0)$ in the continuous spectrum. We consider the two cases separately.

Isolated eigenvalue if $\mu_0 \in (c, \infty)$. Since $\tanh(\mu_0 x_0) = -1 + 2\,\mathrm{e}^{2\mu_0 x_0} + \mathcal{O}(\mathrm{e}^{4\mu_0 x_0})$ as $x_0 \to -\infty$, the simple root of equation (3.8) can be extended asymptotically as follows:

$$k = i\mu_0 \left[1 - 2 \left(\frac{\varkappa_0 - i\mu_0}{\varkappa_0 + i\mu_0} \right) \mathrm{e}^{2\mu_0 x_0} + \mathcal{O}(\mathrm{e}^{4\mu_0 x_0}) \right], \tag{3.9}$$

where $\varkappa_0 := i\sqrt{\mu_0^2 - c^2}$ if $\mu_0 > c$. Therefore, $k \in i\mathbb{R}$ in the first two terms. Similarly, the expansion for $\varkappa = \sqrt{c^2 + k^2}$ is given by

$$\varkappa = \varkappa_0 \left[1 - \frac{2\mu_0^2}{\mu_0^2 - c^2} \mathrm{e}^{2\mu_0 x_0} \left(\frac{\varkappa_0 - i\mu_0}{\varkappa_0 + i\mu_0} \right) + \mathcal{O}(\mathrm{e}^{4\mu_0 x_0}) \right], \tag{3.10}$$

so that $\varkappa \in i\mathbb{R}$ in the first two terms. To show that $k, \varkappa \in i\mathbb{R}$ persists beyond the first two terms, we substitute $k = i\mu$ and $\varkappa = i\nu$ with $\nu = \sqrt{\mu^2 - c^2}$ into (3.8) and obtain the real-valued equation $F(\mu, \alpha) = 0$, where

$$F(\mu, \alpha) := \mu\sqrt{\mu^2 - c^2} - \mu_0^2 + \mu_0(\sqrt{\mu^2 - c^2} - \mu)\alpha, \quad \alpha := \tanh(\mu_0 x_0). \tag{3.11}$$

The function $F(\mu, \alpha) : \mathbb{R}^2 \mapsto \mathbb{R}$ is a C^1 function near $(\mu, \alpha) = (\mu_0, -1)$ satisfying $F(\mu_0, -1) = 0$ and

$$\partial_\mu F(\mu_0, -1) = \sqrt{\mu_0^2 - c^2} + \mu_0 \neq 0.$$

By the implicit function theorem, there exists a simple real root $\mu \in (c, \infty)$ of $F(\mu, \alpha) = 0$ for every $x_0 \ll -1$ ($\alpha \approx -1$) such that $\mu \to \mu_0$ as $x_0 \to -\infty$ ($\alpha \to -1$). Since $k = i\mu \in i\mathbb{R}$ and $\varkappa = i\sqrt{\mu^2 - c^2} \in i\mathbb{R}$, the simple real root $\mu \in (c, \infty)$ determines an isolated eigenvalue $\lambda = -\mu^2 \in (-\infty, -c^2)$ of the spectral problem (1.3).

Resonant pole if $\mu_0 \in (0, c)$. In this case, we have $\varkappa_0 = \sqrt{c^2 - \mu_0^2} \in \mathbb{R}$ so that k and $\varkappa$ in (3.9) and (3.10) are no longer purely imaginary. Since

$$\frac{\varkappa_0 - i\mu_0}{\varkappa_0 + i\mu_0} = \frac{(\varkappa_0 - i\mu_0)^2}{\varkappa_0^2 + \mu_0^2} = \frac{1}{c^2}(c^2 - 2\mu_0^2 - 2i\mu_0\varkappa_0),$$

we obtain from (3.9) and (3.10) that

$$\mathrm{Re}(k) = -\frac{4\mu_0^2}{c^2}\sqrt{c^2 - \mu_0^2}\,\mathrm{e}^{2\mu_0 x_0} + \mathcal{O}(\mathrm{e}^{4\mu_0 x_0})$$

and

$$\mathrm{Im}(\varkappa) = -\frac{4\mu_0^3}{c^2}\,\mathrm{e}^{2\mu_0 x_0} + \mathcal{O}(\mathrm{e}^{4\mu_0 x_0}).$$

Hence, $\mathrm{Re}(k) < 0$ and $\mathrm{Im}(\varkappa) < 0$ for the root of the complex-valued equation $F(\mu, \alpha) = 0$, which still exists for $x_0 \ll -1$ by the same application of the implicit function theorem. Therefore, the eigenfunction $\phi(x; k)$ for this root k satisfies $\phi(x; k) \to 0$ as $x \to -\infty$ because $\mathrm{Im}(k) > 0$, but $\phi(x; k) = b_0\psi(x; k) \to \infty$ as $x \to +\infty$ because $\mathrm{Im}(\varkappa) < 0$. Thus, this root corresponds to the resonant pole $\lambda = k^2$ with $\mathrm{Re}(\lambda) \in (-c^2, 0)$ and $\mathrm{Im}(\lambda) < 0$, for which the eigenfunction $\phi(x; k)$ decays exponentially at $-\infty$ and diverges exponentially at $+\infty$. ∎

Remark 3.4. There exists a symmetric resonant pole $-\bar{k}$ relative to $i\mathbb{R}$ if $\varkappa = -\sqrt{c^2 + k^2}$ is defined according to the second branch of the square root function. The corresponding eigenfunction is associated with the same function $\phi(x; k)$ that decays exponentially at $-\infty$ because $\mathrm{Im}(k) > 0$ but grows exponentially at $+\infty$ as $\phi(x; k) = b_0\psi(x; k)$ because $\mathrm{Re}(k) > 0$, $\mathrm{Re}(\varkappa) < 0$ and $\mathrm{Im}(\varkappa) < 0$.

Remark 3.5. It was missed in ref. [19] that the 'pseudo-embedded eigenvalue' near $\lambda = -\mu_0^2 \in (-c^2, 0)$ splits into a pair of resonant poles. There exists no embedded eigenvalues in the spectral problem (1.3) if $\mu_0 \in (0, c)$.

4. A transmitted soliton via Darboux transformation

The Darboux transformation $u \mapsto \hat{u}$ for the KdV equation (1.1) can be defined as follows [23]. Let u be a bounded solution of the KdV equation (1.1), v_0 be a smooth solution of the linear equations (1.3) and (1.4) with $\lambda_0 \in \mathbb{R}$ and v be an arbitrary solution of the linear equations with arbitrary λ. If $v_0 \neq 0$ everywhere, then

$$\hat{u} := u + 2\frac{\partial^2}{\partial x^2}\log(v_0) \tag{4.1}$$

is a new bounded solution of the KdV equation (1.1) and

$$\hat{v} := \frac{\partial v}{\partial x} - v\frac{\partial}{\partial x}\log(v_0) \tag{4.2}$$

is a solution of the linear equations (1.3) and (1.4) with $u = \hat{u}$ for the same value of λ as in v. Validity of the transformation formulas (4.1) and (4.2) can be checked by direct substitutions.

For the purposes of comparison, we first construct a soliton on the zero background and then study a transmitted soliton on the background of the soliton-free solution satisfying the boundary conditions (1.2).

(a) One soliton on the zero background

For the trivial solution $u = 0$ of the KdV equation (1.1), we can pick the following solution of the linear equations (1.3) and (1.4) with fixed $\lambda_0 = -\mu_0^2 \in (-\infty, 0)$,

$$v_0(t,x) = \mathrm{e}^{\mu_0(x-4\mu_0^2 t - x_0)} + \mathrm{e}^{-\mu_0(x-4\mu_0^2 t - x_0)},$$

where x_0 is arbitrary. Substituting v_0 into (4.1) yields the one-soliton solution

$$\hat{u}(t,x) = 2\mu_0^2\,\mathrm{sech}^2[\mu_0(x - 4\mu_0^2 t - x_0)], \tag{4.3}$$

where μ_0 determines the amplitude $2\mu_0^2$, the width μ_0^{-1} and the velocity $4\mu_0^2$ of the soliton, and x_0 determines the initial location of the soliton. The transformation formula (4.2) for the second, linear independent solution

$$v(t,x) = \mathrm{e}^{\mu_0(x-4\mu_0^2 t - x_0)} - \mathrm{e}^{-\mu_0(x-4\mu_0^2 t - x_0)}$$

of the same linear equations (1.3) and (1.4) with $u = 0$ and $\lambda = \lambda_0$ yields the exponentially decaying solution

$$\hat{v}(t,x) = 2\mu_0 \mathrm{sech}[\mu_0(x - 4\mu_0^2 t - x_0)]$$

of the linear equations (1.3) and (1.4) with $u = \hat{u}$ and $\lambda = \lambda_0$. Hence, $\lambda_0 = -\mu_0^2$ is the isolated eigenvalue of the stationary Schrödinger equation (1.3) corresponding to the one-soliton solution (4.3).

Remark 4.1. Picking solutions of the linear equations (1.3) and (1.4) with fixed $\lambda_0 = k_0^2 \in (0, \infty)$ does not generate bounded solutions of the KdV equation (1.1) by the Darboux transformation. Indeed, a general solution is given by

$$v_0(t,x) = c_1\cos(k_0 x + 4k_0^3 t) + c_2\sin(k_0 x + 4k_0^3 t),$$

where (c_1, c_2) are arbitrary constants. Substituting v_0 into (4.1) yields a new solution of the KdV equation (1.1),

$$\hat{u}(t,x) = -\frac{2k_0^2(c_1^2 + c_2^2)}{[c_1\cos(k_0 x + 4k_0^3 t) + c_2\sin(k_0 x + 4k_0^3 t)]^2},$$

which is singular at countably many lines in the (x,t) plane, where

$$\tan(k_0 x + 4k_0^3 t) = -\frac{c_1}{c_2}.$$

(b) One-soliton on the step function

The following proposition presents the main result of this section. It states that a transmitted soliton can be generated via Darboux transformation.

Proposition 4.2. *Let u be a bounded solution of the KdV equation* (1.1) *with the boundary conditions* (1.2) *such that the spectrum of the Schrödinger equation* (1.3) *is purely continuous in* $[-c^2, \infty)$. *For every* $\lambda_0 < -c^2$, *there exists a choice of a smooth function* v_0 *for which the Darboux transformation* (4.1) *returns a bounded solution* $\hat{u}$ *of the KdV equation* (1.1) *such that the spectrum of the Schrödinger equation* (1.3) *consists of the purely continuous spectrum in* $[-c^2, \infty)$ *and a simple isolated eigenvalue* λ_0.

Proof. Let λ_0 be fixed, so that $\lambda_0 = -\mu_0^2 \in (-\infty, -c^2)$, with $\mu_0 \in (c, \infty)$. Then for $a(t; \mu_0) \neq 0$, there exists a solution $\phi(t, x; \mu_0)$ of the linear system (1.3) and (1.4) satisfying the boundary behaviour (2.7) so that $\phi(t, x; \mu_0) \to 0$ as $x \to -\infty$ and $\phi(t, x; \mu_0) \to \infty$ as $x \to +\infty$. By the Sturm's theorem, $\phi(t, x; \mu_0) > 0$ for every (t, x) since λ_0 is below the spectrum of the Schrödinger equation (1.3) for every $t \in \mathbb{R}$. Similarly, there exists a strictly positive solution $\psi(t, x; \mu_0)$ satisfying $\psi(t, x; \mu_0) \to 0$ as $x \to +\infty$ and $\psi(t, x; \mu_0) \to \infty$ as $x \to -\infty$. If c_1 and c_2 are positive constants,

$$v_0(t, x) = c_1 \phi(t, x; \mu_0) + c_2 \psi(t, x; \mu_0)$$

is positive everywhere so that the Darboux transformation (4.1) yields a bounded solution $\hat{u}$. Let d_1 and d_2 be arbitrary satisfying $c_1 d_2 - c_2 d_1 \neq 0$ and define

$$v(t, x) = d_1 \phi(t, x; \mu_0) + d_2 \psi(t, x; \mu_0).$$

Due to the decay and divergence conditions on $\phi(t, x; \mu_0)$ and $\psi(t, x; \mu_0)$, the transformation (4.2) yields an exponentially decaying solution

$$\hat{v} = (c_1 d_2 - c_2 d_1) \frac{(\phi(t, x; \mu_0) \partial_x \psi(t, x; \mu_0) - \psi(t, x; \mu_0) \partial_x \phi(t, x; \mu_0))}{c_1 \phi(t, x; \mu_0) + c_2 \psi(t, x; \mu_0)},$$

of the Schrödinger equation (1.3) for $\lambda = \lambda_0$. Hence, $\lambda_0 \in (-\infty, -c^2)$ is an isolated eigenvalue. It is a simple eigenvalue by the Sturm theorem. For every other value of λ, the transformation (4.2) returns bounded oscillatory solutions if $\lambda \in [-c^2, \infty)$ and unbounded solutions if $\lambda \in (-\infty, -c^2) \backslash \{\lambda_0\}$ so that the spectrum of the Schrödinger equation (1.3) associated with $\hat{u}$ consists of the purely continuous spectrum in $[-c^2, \infty)$ and a simple isolated eigenvalue λ_0. ∎

We illustrate the Darboux transformation for the transmitted soliton by considering an example with the initial data $u_0(x) = c^2 H(x)$ at $t = 0$, and drop t from the list of arguments. We use the following solution of the stationary Schrödinger equation (1.3) with $u = u_0$ and $\lambda = -\mu_0^2 \in (-\infty, -c^2)$ with $\mu_0 \in (c, \infty)$,

$$v_0(x) = \begin{cases} \mathrm{e}^{\mu_0 (x - x_0)} + \mathrm{e}^{-\mu_0 (x - x_0)}, & x < 0, \\ c_1 \, \mathrm{e}^{\nu_0 x} + c_2 \, \mathrm{e}^{-\nu_0 x}, & x > 0, \end{cases}$$

where $\nu_0 := \sqrt{\mu_0^2 - c^2} > 0$, x_0 is arbitrary, and (c_1, c_2) are found from the continuity of v_0 and v_0' across $x = 0$. Setting up and solving the linear system for (c_1, c_2) similar to (3.1), we obtain the unique solution:

$$\begin{cases} c_1 = \dfrac{\nu_0 + \mu_0}{2\nu_0} \, \mathrm{e}^{-\mu_0 x_0} + \dfrac{\nu_0 - \mu_0}{2\nu_0} \, \mathrm{e}^{\mu_0 x_0}, \\ c_2 = \dfrac{\nu_0 - \mu_0}{2\nu_0} \, \mathrm{e}^{-\mu_0 x_0} + \dfrac{\nu_0 + \mu_0}{2\nu_0} \, \mathrm{e}^{\mu_0 x_0}. \end{cases}$$

Substituting v_0 into (4.1) yields the initial condition, where one soliton is superposed to the step function:

$$\hat{u}_0(x) = 2\mu_0^2 \operatorname{sech}^2[\mu_0 (x - x_0)], \quad x < 0 \tag{4.4}$$

and

$$\hat{u}_0(x) = c^2 + 4\nu_0^2 \frac{\nu_0^2 + \mu_0^2 + (\nu_0^2 - \mu_0^2) \cosh(2\mu_0 x_0)}{[(\nu_0 + \mu_0) \cosh(\nu_0 x - \mu_0 x_0) + (\nu_0 - \mu_0) \cosh(\nu_0 x + \mu_0 x_0)]^2}, \tag{4.5}$$

for $x > 0$. The denominator of (4.5) is strictly positive for every $x_0 \in (-\infty, x_*)$, where x_* is the unique positive root of the transcendental equation:

$$\cosh(2\mu_0 x_0) = \frac{\mu_0 + \nu_0}{\mu_0 - \nu_0} > 1.$$

If $x_0 = x_*$, the expression (4.5) is singular at $x = \mu_0 x_0/\nu_0$, and if $x_0 \in (x_*, \infty)$, there exist two singularities of (4.5) on $(0, \infty)$ before and after the value $x = \mu_0 x_0/\nu_0$. The transmitted soliton corresponds to the value of x_0 inside $(-\infty, x_*)$.

Remark 4.3. The one-soliton $\hat{u}_0$ decays differently as $x \to -\infty$ and as $x \to +\infty$, according to (4.4) and (4.5). The decay rate μ_0 at $-\infty$ corresponds to the zero boundary condition, whereas the decay rate $\nu_0 = \sqrt{\mu_0^2 - c^2}$ at $+\infty$ corresponds to the non-zero boundary condition c^2. Due to this discrepancy, the one-soliton obtained by the Darboux transformation is different from the initial condition (3.5), which has the same decay rate μ_0 at $\pm\infty$. In addition, the former is related to the isolated eigenvalue $\lambda_0 = -\mu_0^2$, whereas the latter is related to the isolated eigenvalue $\lambda = k_0^2$ with $k_0 = i\mu_0 + \mathcal{O}(e^{2\mu_0 x_0})$ given by (3.9).

Remark 4.4. The one-soliton $\hat{u}_0$ given by (4.4) and (4.5) corresponds to the initial condition for the transmitted soliton which overtakes the RW in the time dynamics of the KdV equation (1.1). The corresponding time-dependent solution can be constructed from the Darboux transformation with the RW solution $u = u(t, x)$. Since solutions $u(t, x)$ and $v_0(t, x)$ are not explicit, we do not obtain $\hat{u}(t, x)$ in the explicit form for $t \neq 0$.

Remark 4.5. If $\lambda = -\mu_0^2 \in (-c^2, 0)$ with $\mu_0 \in (0, c)$, solution of the stationary Schrödinger equation (1.3) is a bounded and oscillatory function for $x > 0$. Darboux transformation (4.1) generates unbounded solution $\hat{u}_0(x)$ at a countable set of points for $x > 0$ similarly to remark 4.1. No trapped soliton can be constructed by the Darboux transformation for $\lambda \in (-c^2, 0)$ because no embedded eigenvalues with spatially decaying eigenfunctions exist.

Remark 4.6. If $\lambda = k_0^2 \in (0, \infty)$, then solutions of the stationary Schrödinger equation (1.3) are bounded and oscillatory for both $x < 0$ and $x > 0$. Darboux transformation (4.1) generates unbounded solution $\hat{u}_0(x)$ at countable sets of points for both $x < 0$ and $x > 0$.

5. Time dynamics of one-soliton on the RW background

Here, we perform the time-dependent computations of the KdV equation (1.1). We utilize here the finite-difference method introduced by Zabusky and Kruskal in [24] for numerical solution of the KdV equation (1.1).

Let u_n^m be a numerical approximation of $u(t_m, x_n)$ on the equally spaced grid $\{x_n\}$ with the equally space times $\{t_m\}$. The time step is τ, and the spatial step size is h. The two-point numerical method in ref. [24] is given by

$$u_n^{m+1} = u_n^{m-1} - \frac{2\tau}{h}\left(u_{n+1}^m + u_n^m + u_{n-1}^m\right)\left(u_{n+1}^m - u_{n-1}^m\right) - \frac{\tau}{h^3}\left(u_{n+2}^m - 2u_{n+1}^m + 2u_{n-1}^m - u_{n-2}^m\right).$$

The first step is performed separately with the Euler method

$$u_n^1 = u_n^0 - \frac{\tau}{h}\left(u_{n+1}^0 + u_n^0 + u_{n-1}^0\right)\left(u_{n+1}^0 - u_{n-1}^0\right) - \frac{\tau}{2h^3}\left(u_{n+2}^0 - 2u_{n+1}^0 + 2u_{n-1}^0 - u_{n-2}^0\right).$$

The finite-difference method is stable if $\tau < 2/3\sqrt{3}h^3$ for small h [24]. To avoid oscillations of solutions due to the step background, we use the smooth function (3.4) superposed with the soliton (3.5) so that the initial data are

$$u_0(x) = 2\mu_0^2 \operatorname{sech}^2(\mu_0(x - x_0)) + \frac{1}{2}c^2\left[1 + \tanh(\varepsilon x)\right], \tag{5.1}$$

where $x_0 < 0$ and $\varepsilon = 1$.

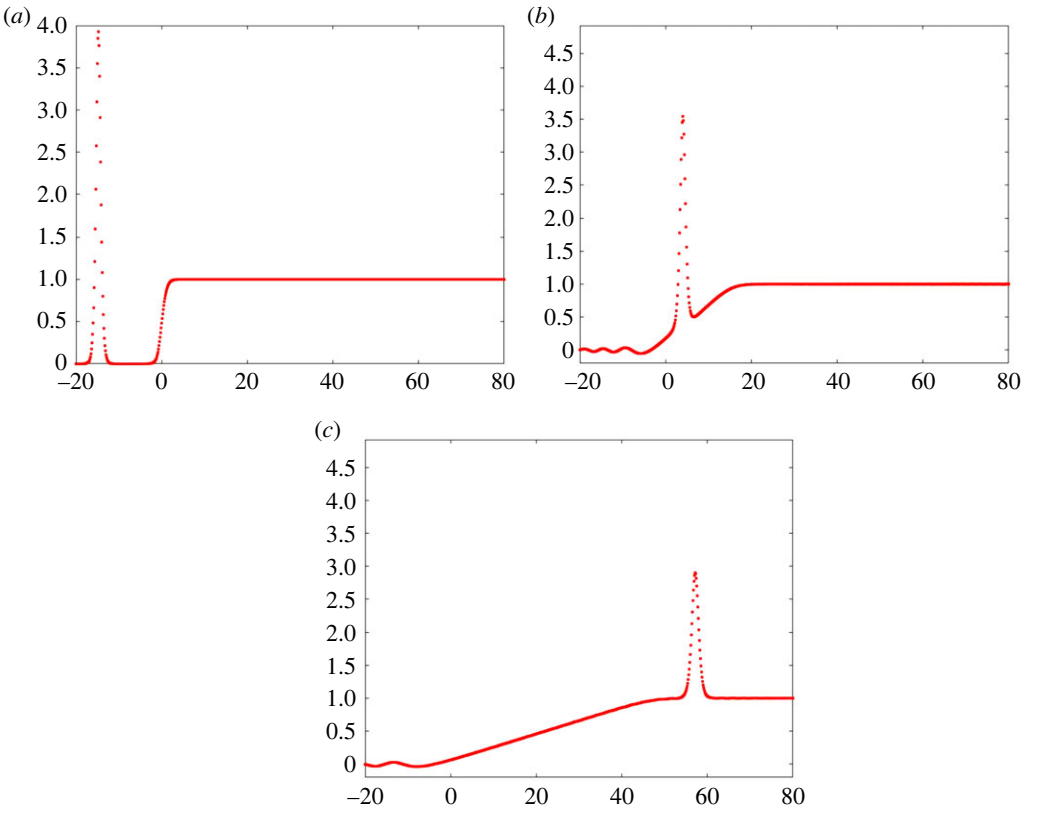

Figure 1. The time evolution of a transmitted soliton for $\mu = 1.4, c = 1, x_0 = -15$ and $\varepsilon = 1$ at (*a*) $t = 0$, (*b*) $t = 4$ and (*c*) $t = 8$. (Online version in colour.)

(a) Outcomes of numerical computations

Evolution of the KdV equation (1.1) with the initial data (5.1) depends on the amplitude of $2\mu_0^2$ of the solitary wave to the left of the step-like background. Figure 1 shows three snapshots of the evolution with $\mu_0 = 1.4 > c = 1$. A travelling solitary wave with a sufficiently large amplitude reaches and overtakes the RW formed from the step-like background. This corresponds to dynamics of the transmitted soliton.

Figure 2 shows three snapshots of the evolution with $\mu_0 = 0.95 < c = 1$. A travelling solitary wave with a sufficiently small amplitude becomes trapped inside the RW and does not reach its top. This corresponds to dynamics of the trapped soliton.

The different behaviour on figures 1 and 2 is related to the different spectrum of the stationary Schrödinger equation (1.3) shown on figure 3. We compute the spectrum by using the second-order central-difference approximation for the Schrödinger equation (1.3) with the potential (5.1). Figure 3*a* shows the spectrum for $\mu = 1.4$. The isolated eigenvalue is superimposed with the approximation obtained from the numerically computed root of the function (3.11). The difference between the two approximations is not visible on the scale of the figure, and it is of the order of $\mathcal{O}(10^{-3})$. Figure 3*b* shows the spectrum for $\mu = 0.95$, for which no isolated or embedded eigenvalues exist.

(b) Data analysis

We will elaborate the numerical criterion to show that the trapped soliton disappears in the long-time dynamics of the RW. In other words, the solitary wave does not appear to be a proper soliton on the RW background but is instead completely absorbed by the RW.

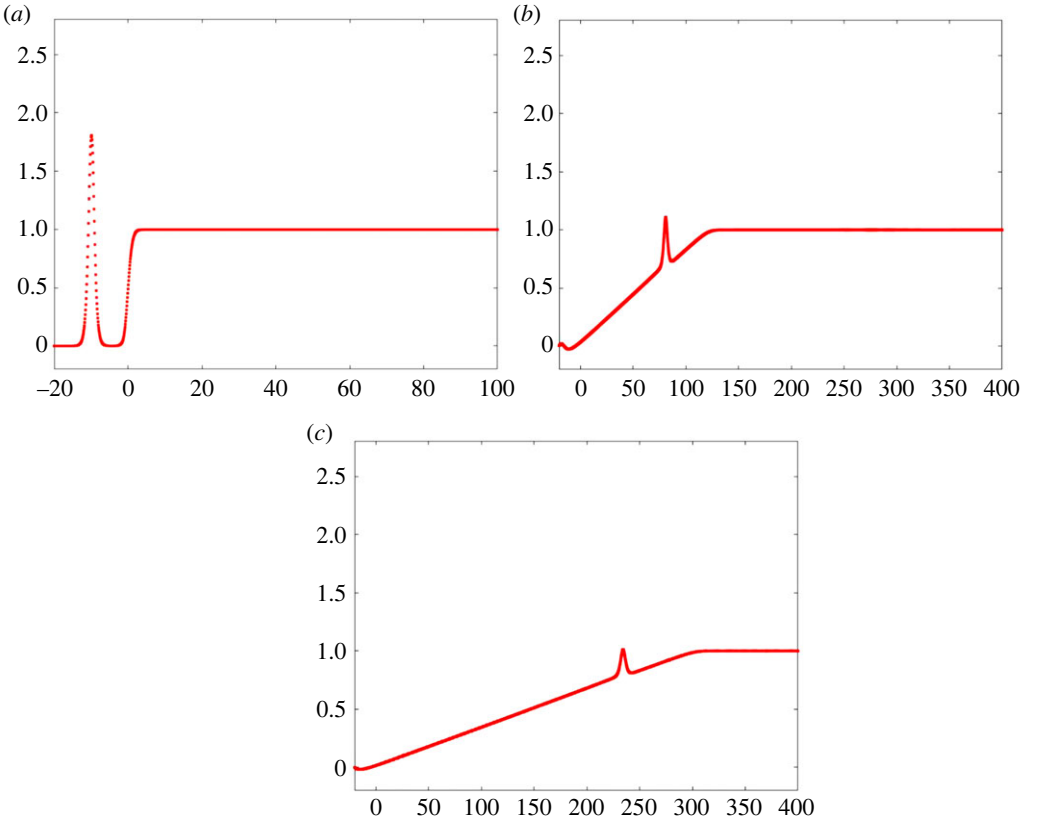

Figure 2. The time evolution of a trapped soliton for $\mu = 0.95$, $c = 1$, $x_0 = -10$ and $\varepsilon = 1$ at (*a*) $t = 0$, (*b*) $t = 20$ and (*c*) $t = 40$. (Online version in colour.)

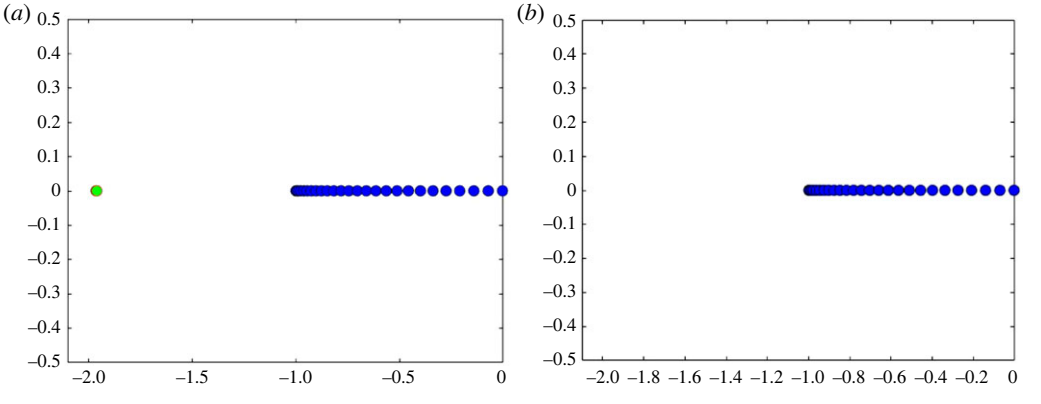

Figure 3. Spectrum of the stationary Schrödinger equation (1.3) for (*a*) $\mu = 1.4$ and (*b*) $\mu = 0.95$ with the potential u_0 given by (5.1). (Online version in colour.)

Let a^2 be the constant background (which may change in time). The solitary wave on the constant background is obtained from the soliton on the zero background (4.3) with the Galilean transformation:

$$u(t,x) = a^2 + 2\nu_0^2 \operatorname{sech}^2[\nu_0(x - 4\nu_0^2 t - 6a^2 t - x_0)], \tag{5.2}$$

where $\nu_0 > 0$ is the soliton parameter. As follows from the construction of one-soliton on the constant background with the Darboux transformation, see expressions (4.4) and (4.5), ν_0 is related to the fixed value μ_0 (determined for $a = 0$) by $\nu_0 = \sqrt{\mu_0^2 - a^2}$ as long as $a < \mu_0$. Hence, the amplitude of the soliton (5.2) on the constant background a^2 is expressed as follows:

$$A = a^2 + 2\nu_0^2 = 2\mu_0^2 - a^2.$$

When the solitary wave advances to the RW from the left and is strongly localized on the long scale of the RW like on figures 1 and 2, the background a^2 is determined by the value of the RW at the location of the solitary wave.

The RW background can be approximated by the solution of the inviscid Burgers' equation $u_t + 6uu_x = 0$ starting with the piecewise linear profile:

$$u_0(x) = \begin{cases} 0, & x < -\varepsilon, \\ (2\varepsilon)^{-1}(x+\varepsilon), & -\varepsilon \le x \le \varepsilon, \\ 1, & x > \varepsilon. \end{cases}$$

Solving the inviscid Burgers' equation with $u(0,x) = u_0(x)$ yields

$$u(t,x) = \begin{cases} 0, & x < -\varepsilon, \\ (2\varepsilon + 6t)^{-1}(x+\varepsilon), & -\varepsilon \le x \le \varepsilon + 6t, \\ 1, & x > \varepsilon + 6t. \end{cases}$$

Location $\xi(t)$ of the solitary wave on the RW is detected numerically from which we determine

$$a^2(t) = (2\varepsilon + 6t)^{-1}(\xi(t) + \varepsilon) \quad \text{as long as } \xi(t) \in [-\varepsilon, \varepsilon + 6t].$$

This gives the theoretical prediction of the amplitude of the solitary wave,

$$A(t) = 2\mu_0^2 - a^2(t).$$

The theoretical prediction can be compared with the numerical approximation of the amplitude of the solitary wave computed by the quadratic interpolation from three grid points near the maximum of u.

Figure 4 shows the numerically detected amplitude of the solitary wave versus time (figure 4*a*) and versus the amplitude of the RW background (figure 4*b*) for the transmitted soliton with $\mu_0 = 1.4 > c = 1$. The numerical approximation is shown by the black solid line. The red dashed line show the final amplitude $A_\infty = 2\mu_0^2 - c^2$ (figure 4*a*) and the theoretically computed amplitude $A(t) = 2\mu_0^2 - a^2(t)$ (figure 4*b*). It is obvious that the discrepancy between the two lines disappear with time and that $A(t) \to A_\infty$ as t evolves. The blue dashed line on figure 4*b* shows the amplitude of the background $a^2(t)$ at the location of the transmitted soliton. Since $a^2(t) \to c^2$ and $A_\infty > c^2$ since $\mu_0 = 1.4 > c = 1$, the black solid line and the blue dashed line do not meet and the soliton is transmitted over the RW background as shown in figure 1.

Figure 5 shows the same quantities as shown in figure 4 but for the trapped soliton with $\mu_0 = 0.95 < c = 1$. Since $A_\infty = 2\mu_0^2 - c^2 < c^2$, the amplitude of the solitary wave never reaches the horizontal asymptote on figure 5*a* because the trapped soliton dissolves inside the RW. Figure 5*b* shows again that the numerical approximation (black solid line) is getting closer to the theoretical approximation of the soliton amplitude $A(t)$ (red dashed line) as t evolves. However, for the trapped soliton, the black solid line and the blue dashed line meet so that there exists the limiting value of the background a_∞^2 such that $a(t) \to a_\infty$ as $t \to \infty$. The limiting value a_∞ is found from the balance $2\mu_0^2 - a_\infty^2 = a_\infty^2$ at $a_\infty = \mu_0$. Hence, the trapped solitary wave completely disappears inside the RW background as shown in figure 2.

6. Summary

We have considered the case when a solitary wave is added on the step-like initial data for the KdV equation. The step-like initial data evolve into a RW, whereas the solitary wave either

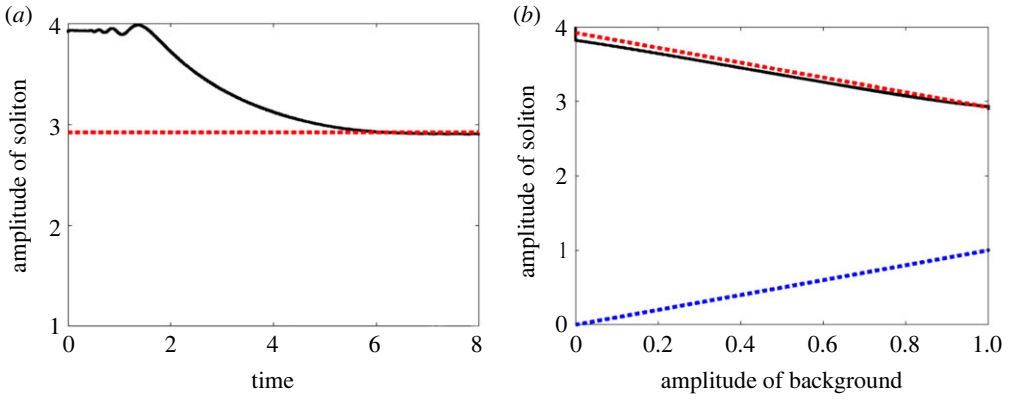

Figure 4. Data analysis for the transmitted soliton shown in figure 1: (*a*) amplitude of the solitary wave versus time (black) and the limiting amplitude $A_\infty = 2\mu_0^2 - c^2$ (red). (*b*) Amplitude of the solitary wave versus amplitude of the RW background detected numerically (black) and theoretically (red). The blue dashed line shows the amplitude of the RW background. (Online version in colour.)

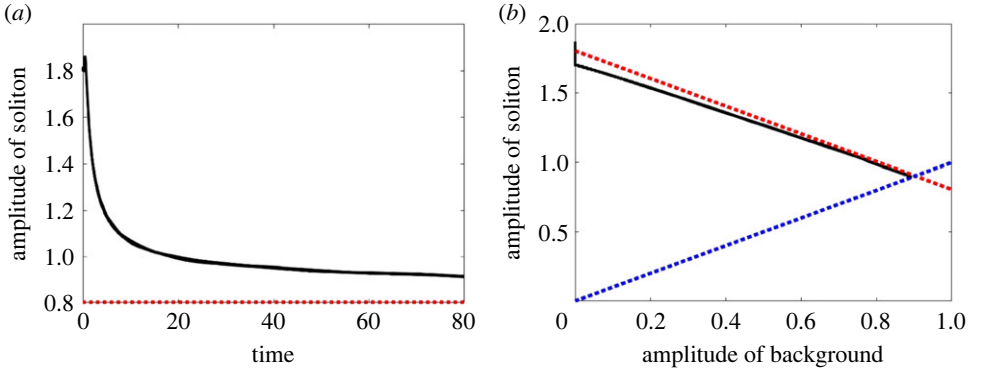

Figure 5. The same as shown in figure 4 but for the trapped soliton shown in figure 2. (Online version in colour.)

propagates over the RW or completely disappears inside the RW. The outcome depends on whether there exists an isolated eigenvalue of the Schrödinger spectral problem outside the continuous spectrum. If it exists, we can construct the transmitted soliton by using the Darboux transformation. If the isolated eigenvalue does not exist, we have shown that no embedded eigenvalues exist because zeros of the transmission coefficients that correspond to the soliton data transform into complex resonant poles.

We hope that this study will open a road for further advances on the subject of solitary waves propagating over the RW and DSW backgrounds. One of the important problems is to use the Darboux transformation for computations of the limiting phase shifts of the transmitted solitary waves as $t \to \pm\infty$ and comparison with the experimentally detected phase shifts [4]. Another interesting problem is to understand better how the modulation theory for soliton propagation used in our data analysis is justified within the Whitham modulation theory [9–11]. Although the resolution formulas for N solitons transmitted over the zero background have been derived in refs. [20,21], it is interesting to see how the transformations between the two problems change these formulas to the case of the non-zero boundary conditions and how these formulas correspond to outcomes of the qualitative theory of soliton tunnelling in refs. [5,6].

Data accessibility. The authors declare that the data is available upon request.

Authors' contributions. A.M.: formal analysis, validation, visualization and writing—original draft; D.P.: conceptualization, formal analysis, project administration, supervision, writing—review and editing.

All authors gave final approval for publication and agreed to be held accountable for the work performed therein.

Conflict of interest declaration. The authors declare that they have no conflict of interest.

Funding. The project is supported by the RSF grant no. 19-12-00253.

Acknowledgements. The authors thank M.A. Hoefer for guidance during the project as well as G.El and A. Rybkin for useful suggestions.

References

1. Ablowitz MJ. 2011 *Nonlinear dispersive waves: asymptotic analysis and solitons*. Cambridge: Cambridge University Press.
2. El GA. 2007 Korteweg-de Vries equation: solitons and undular bores. *Solitary waves in fluids*. *Adv. Fluid Mech.* **47**, 19–53. (WIT Press, Southampton, 2007)
3. El GA, Hoefer MA. 2016 Dispersive shock waves and modulation theory. *Physica D* **333**, 11–65. (doi:10.1016/j.physd.2016.04.006)
4. Maiden MD, Anderson DV, Franco AA, El GA, Hoefer MA. 2018 Solitonic dispersive hydrodynamics: theory and observation. *Phys. Rev. Lett.* **120**, 144101. (doi:10.1103/PhysRevLett.120.144101)
5. Sprenger P, Hoefer MA, El GA. 2018 Hydrodynamic optical soliton tunneling. *Phys. Rev. E* **97**, 032218. (doi:10.1103/PhysRevE.97.032218)
6. van der Sande K, El GA, Hoefer MA. 2021 Dynamic soliton–mean flow interaction with non-convex flux. *J. Fluid Mech.* **928**, A21. (doi:10.1017/jfm.2021.803)
7. Gavrilyuk S, Shyue KM. 2022 Singular solutions of the BBM equation: analytical and numerical study. *Nonlinearity* **35**, 388–410. (doi:10.1088/1361-6544/ac3921)
8. Congy T, El GA, Hoefer MA. 2019 Interaction of linear modulated waves and unsteady dispersive hydrodynamic states with application to shallow water waves. *J. Fluid Mech.* **875**, 1145–1174. (doi:10.1017/jfm.2019.534)
9. Clarke WA, Marangell R. 2021 Rigorous justification of the Whitham modulation theory for equations of NLS type. *Stud. Appl. Math.* **147**, 577–621. (doi:10.1111/sapm.12390)
10. Wang DS, Xu L, Xuan Z. 2022 The complete classification of solutions to the Riemann problem of the defocusing complex modified KdV equation. *J. Nonlinear Sci.* **32**, 3. (doi:10.1007/s00332-021-09766-6)
11. Liu Y, Wang DS. 2022 Exotic wave patterns in Riemann problem of the high-order Jaulent–Miodek equation: Whitham modulation theory. *Stud. Appl. Math.* **149**, 588–630. (doi:10.1111/sapm.12513)
12. Biondini G, Li S, Mantzavinos D. 2018 Soliton trapping, transmission, and wake in modulationally unstable media. *Phys. Rev. E* **98**, 042211. (doi:10.1103/PhysRevE.98.042211)
13. Biondini G, Li S, Mantzavinos D. 2021 Long-time asymptotics for the Focusing nonlinear Schrödinger equation with nonzero boundary conditions in the presence of a discrete spectrum. *Commun. Math. Phys.* **382**, 1495–1577. (doi:10.1007/s00220-021-03968-5)
14. Grava T, Minakov A. 2020 On the long-time asymptotic behavior of the modified Korteweg–de Vries equation with step-like initial data. *SIAM J. Math. Anal.* **52**, 5892–5993. (doi:10.1137/19M1279964)
15. Novikov SP, Manakov SV, Pitaevskii LP, Zakharov VE. 1984 *Theory of solitons: the inverse scattering method*. New York: Consultants Bureau.
16. Gardner CS, Greene JM, Kruskal MD, Miura RM. 1967 Method for solving the Korteweg-de Vries equation. *Phys. Rev. Lett.* **19**, 1095–1097. (doi:10.1103/PhysRevLett.19.1095)
17. Lax PD. 1968 Integrals of nonlinear equations of evolution and solitary waves. *Comm. Pure Appl. Math.* **21**, 467–490. (doi:10.1002/cpa.3160210503)
18. Deift P, Trubowitz E. 1979 Inverse scattering on the line. *Commun. Pure Appl. Math.* **32**, 121–251. (doi:10.1002/cpa.3160320202)
19. Ablowitz MJ, Luo XD, Cole JT. 2018 Solitons, the Korteweg–de Vries equation with step boundary values, and pseudo-embedded eigenvalues. *J. Math. Phys.* **59**, 091406. (doi:10.1063/1.5026332)

20. Egorova I, Gladka Z, Kotlyarov V, Teschl G. 2013 Long-time asymptotics for the Korteweg–de Vries equation with steplike initial data. *Nonlinearity* **26**, 1839–1864. (doi:10.1088/0951-7715/26/7/1839)
21. Egorova I, Michor J, Teschl G. 2022 Soliton asymptotics for the KdV shock waves via classical inverse scattering. *J. Math. Anal. Appl.* **514**, 126251. (https://doi.org/10.1016/j.jmaa.2022.126251)
22. Morse P.M, Feshbach H. 1953 *Methods of theoretical physics*, vol. I. New York: McGraw–Hill Book Company Inc.
23. Matveev VB, Salle MA. 1991 *Darboux transformations and solitons*. Berlin: Springer-Verlag.
24. Zabusky NJ, Kruskal MD. 1965 Interaction of 'solitons' in a collisionless plasma and the recurrence of initial states. *Phys. Rev. Lett.* **15**, 240–243. (doi:10.1103/PhysRevLett.15.240)